

University of Wollongong

Research Online

---

Australian Institute for Innovative Materials -  
Papers

Australian Institute for Innovative Materials

---

1-1-2017

## Origin of thermally stable ferroelectricity in a porous barium titanate thin film synthesized through block copolymer templating

Norihiro Suzuki

*National Institute for Materials Science, Japan*

Minoru Osada

*National Institute for Materials Science, Japan*

Md Motasim Billah

*University of Wollongong, National Institute for Materials Science, Japan, mmb959@uowmail.edu.au*

Zeid Abdullah Allothman

*King Saud University*

Yoshio Bando

*National Institute for Materials Science, Japan, University of Wollongong, BANDO.Yoshio@nims.go.jp*

*See next page for additional authors*

Follow this and additional works at: <https://ro.uow.edu.au/aiimpapers>



Part of the [Engineering Commons](#), and the [Physical Sciences and Mathematics Commons](#)

---

Research Online is the open access institutional repository for the University of Wollongong. For further information contact the UOW Library: [research-pubs@uow.edu.au](mailto:research-pubs@uow.edu.au)

---

# Origin of thermally stable ferroelectricity in a porous barium titanate thin film synthesized through block copolymer templating

## Abstract

A porous barium titanate ( $\text{BaTiO}_3$ ) thin film was chemically synthesized using a surfactant-assisted sol-gel method in which micelles of amphiphathic diblock copolymers served as structure-directing agents. In the Raman spectrum of the porous  $\text{BaTiO}_3$  thin film, a peak corresponding to the ferroelectric tetragonal phase was observed at around  $710 \text{ cm}^{-1}$ , and it remained stable at much higher temperature than the Curie temperature of bulk single-crystal  $\text{BaTiO}_3$  ( $\sim 130^\circ\text{C}$ ). Measurements revealed that the ferroelectricity of the  $\text{BaTiO}_3$  thin film has high thermal stability. By analyzing high-resolution transmission electron microscope images of the  $\text{BaTiO}_3$  thin film by the fast Fourier transform mapping method, the spatial distribution of stress in the  $\text{BaTiO}_3$  framework was clearly visualized. Careful analysis also indicated that the porosity in the  $\text{BaTiO}_3$  thin film introduced anisotropic compressive stress, which deformed the crystals. The resulting elongated unit cell caused further displacement of the  $\text{Ti}^{4+}$  cation from the center of the lattice. This displacement increased the electric dipole moment of the  $\text{BaTiO}_3$  thin film, effectively enhancing its ferro(piezo)electricity.

## Disciplines

Engineering | Physical Sciences and Mathematics

## Publication Details

Suzuki, N., Osada, M., Billah, M., Allothman, Z. Abdullah., Bando, Y., Yamauchi, Y. & Hossain, M. A. (2017). Origin of thermally stable ferroelectricity in a porous barium titanate thin film synthesized through block copolymer templating. *APL Materials*, 5 (7), 076111-1-076111-7.

## Authors

Norihiro Suzuki, Minoru Osada, Md Motasim Billah, Zeid Abdullah Allothman, Yoshio Bando, Yusuke Yamauchi, and Md. Shahriar Al Hossain

## Origin of thermally stable ferroelectricity in a porous barium titanate thin film synthesized through block copolymer templating

Norihiro Suzuki, Minoru Osada, Motasim Billah, Zeid Abdullah Alothman, Yoshio Bando, Yusuke Yamauchi, and Md. Shahriar A. Hossain

Citation: *APL Materials* **5**, 076111 (2017); doi: 10.1063/1.4995650

View online: <http://dx.doi.org/10.1063/1.4995650>

View Table of Contents: <http://aip.scitation.org/toc/apm/5/7>

Published by the [American Institute of Physics](#)

---

### Articles you may be interested in

[Research Update: Enhancement of figure of merit for energy-harvesters based on free-standing epitaxial  \$\text{Pb}\(\text{Zr}\_{0.52}\text{Ti}\_{0.48}\)\_{0.99}\text{Nb}\_{0.01}\text{O}\_3\$  thin-film cantilevers](#)

*APL Materials* **5**, 074201 (2017); 10.1063/1.4978273

[Domain wall conductivity in  \$\text{KTiOPO}\_4\$  crystals](#)

*APL Materials* **5**, 076108 (2017); 10.1063/1.4995651

[Synthesis and superconductivity of In-doped SnTe nanostructures](#)

*APL Materials* **5**, 076110 (2017); 10.1063/1.4994293

[Enhanced electric polarization and breakdown strength in the all-organic sandwich-structured poly\(vinylidene fluoride\)-based dielectric film for high energy density capacitor](#)

*APL Materials* **5**, 076109 (2017); 10.1063/1.4995653

[High mobility yttrium doped cadmium oxide thin films](#)

*APL Materials* **5**, 076105 (2017); 10.1063/1.4993799

[Sputter synthesis of wafer-scale hexagonal boron nitride films via interface segregation](#)

*APL Materials* **5**, 076107 (2017); 10.1063/1.4995652

---



Running in circles looking for the best **science job?**

Search hundreds of exciting new jobs each month!

**PHYSICS TODAY | JOBS**  
[www.physicstoday.org/jobs](http://www.physicstoday.org/jobs)

## Origin of thermally stable ferroelectricity in a porous barium titanate thin film synthesized through block copolymer templating

Norihiro Suzuki,<sup>1,a,b</sup> Minoru Osada,<sup>2</sup> Motasim Billah,<sup>2,3</sup>  
 Zeid Abdullah Alothman,<sup>4</sup> Yoshio Bando,<sup>2,3</sup> Yusuke Yamauchi,<sup>2,3,4,b</sup>  
 and Md. Shahriar A. Hossain<sup>2,3</sup>

<sup>1</sup>International Center for Young Scientists (ICYS), National Institute for Materials Science (NIMS), 1-2-1 Sengen, Tsukuba, Ibaraki 305-0047, Japan

<sup>2</sup>International Center for Materials Nanoarchitectonics (MANA), National Institute for Materials Science (NIMS), 1-1 Namiki, Tsukuba, Ibaraki 305-0044, Japan

<sup>3</sup>Australian Institute for Innovative Materials (AIIM), University of Wollongong, Squires Way, North Wollongong, NSW 2500, Australia

<sup>4</sup>Advanced Materials Research Chair, Chemistry Department, College of Science, King Saud University, Riyadh 11451, Saudi Arabia

(Received 9 March 2017; accepted 21 June 2017; published online 28 July 2017; publisher error corrected 31 July 2017)

A porous barium titanate ( $\text{BaTiO}_3$ ) thin film was chemically synthesized using a surfactant-assisted sol-gel method in which micelles of amphiphathic diblock copolymers served as structure-directing agents. In the Raman spectrum of the porous  $\text{BaTiO}_3$  thin film, a peak corresponding to the ferroelectric tetragonal phase was observed at around  $710 \text{ cm}^{-1}$ , and it remained stable at much higher temperature than the Curie temperature of bulk single-crystal  $\text{BaTiO}_3$  ( $\sim 130 \text{ }^\circ\text{C}$ ). Measurements revealed that the ferroelectricity of the  $\text{BaTiO}_3$  thin film has high thermal stability. By analyzing high-resolution transmission electron microscope images of the  $\text{BaTiO}_3$  thin film by the fast Fourier transform mapping method, the spatial distribution of stress in the  $\text{BaTiO}_3$  framework was clearly visualized. Careful analysis also indicated that the porosity in the  $\text{BaTiO}_3$  thin film introduced anisotropic compressive stress, which deformed the crystals. The resulting elongated unit cell caused further displacement of the  $\text{Ti}^{4+}$  cation from the center of the lattice. This displacement increased the electric dipole moment of the  $\text{BaTiO}_3$  thin film, effectively enhancing its ferro(piezo)electricity. © 2017 Author(s). All article content, except where otherwise noted, is licensed under a Creative Commons Attribution (CC BY) license (<http://creativecommons.org/licenses/by/4.0/>). [<http://dx.doi.org/10.1063/1.4995650>]

In early 1940s, barium titanate ( $\text{BaTiO}_3$ , hereafter denoted as BT) was the first metal oxide discovered to be a typical perovskite ferroelectric material.<sup>1</sup> BT is still widely used because of its balanced ferroelectric and piezoelectric responses, as well as its favorable coupling factor and dielectric constant. In addition, lead-free BT is an eco-friendly material, so it has drawn great interest as a replacement for lead zirconate titanate. At room temperature, the crystal phase of BT is tetragonal with a ratio of lattice parameters  $c$  to  $a$  ( $c/a$ ) that is not equal to 1. In the tetragonal phase, the BT lattice is slightly distorted, and the cations ( $\text{Ba}^{2+}$ ,  $\text{Ti}^{4+}$ ) and anions ( $\text{O}^{2-}$ ) are displaced in opposite directions. This displacement results in the spontaneous polarization of BT. When the temperature increases to the Curie temperature ( $T_C$ ), the phase transition to the cubic phase occurs. In the cubic phase of BT that has  $c/a = 1$ , the lattice distortion is relaxed, and the ferroelectricity is lost. Because  $T_C$  of BT is relatively low (around  $130 \text{ }^\circ\text{C}$ ), BT is not a suitable ferroelectric material for use at high temperature.

<sup>a</sup>Present Address: Research Institute for Science and Technology, Tokyo University of Science, 2641 Yamazaki, Noda, Chiba 278-8510, Japan.

<sup>b</sup>Electronic addresses: [suzuki.norihiro@rs.tus.ac.jp](mailto:suzuki.norihiro@rs.tus.ac.jp) and [yusuke@uow.edu.au](mailto:yusuke@uow.edu.au)



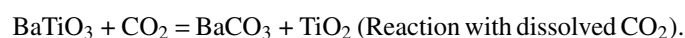
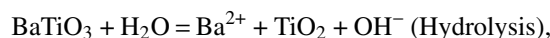
To increase  $T_C$  of BT, the ferroelectric (tetragonal) phase has been stabilized by applying stress at the heterointerface. For example, Choi *et al.*<sup>2</sup> enhanced the ferroelectricity of BT films epitaxially grown on GdScO<sub>3</sub> (110) and DyScO<sub>3</sub> (110) substrates by utilizing the biaxial compressive stress caused by the lattice mismatch. In simple bilayer structures, however, the stress relaxes as the BT film becomes thicker. Thus, the enhancement of  $T_C$  is limited to very thin films (less than ten nanometers thick),<sup>3,4</sup> which are impractical for device applications. To increase the BT film thickness while preventing stress relaxation, a superlattice (periodic structure of very thin layers) and a three-dimensional (3D) heteronanostructure have been developed. Harrington *et al.*<sup>5</sup> synthesized vertical mesostructures of BT and Sm<sub>2</sub>O<sub>3</sub> to obtain micrometer-order thick films with  $T_C$  above 800 °C. Inspired by this study, we chemically synthesized a 3D nanocomposite by introducing a precursor solution of BT onto a mesoporous strontium titanate (SrTiO<sub>3</sub>, hereafter denoted as ST) thin film.<sup>6</sup>  $T_C$  of the resulting ST/BT nanocomposite reached 230 °C.

Our idea is that the curvature of porosity itself creates such stress that it can cause  $T_C$  of a thin film to increase without heterointerfaces. In a previous report, we synthesized mesoporous BT thin films by a surfactant-assisted sol-gel method and found that  $T_C$  of a porous BT thin film increased up to around 470 °C.<sup>7</sup> Such enhancement of  $T_C$  did not occur in a non-porous BT thin film synthesized by the same procedure. In addition, the piezoelectricity of the mesoporous BT film was higher than that of the non-porous one. In this study, we visualize the stress within the porous framework of a mesoporous BT film and clarify the thermal stability of the ferroelectric (tetragonal) phase induced by such stress. It is proved that mesopore-induced stress is the main reason for the enhancement of  $T_C$  of the thin film.

In the experiment, a polystyrene-*b*-poly(ethylene oxide) diblock copolymer [PS(18000)-*b*-PEO(7500)] (50 mg) was dissolved in tetrahydrofuran (THF) (1.5 ml) at 40 °C and then cooled to room temperature. Barium acetate (127.7 mg) was dissolved in 37 wt. % acetic acid (830  $\mu$ l) by stirring at 50 °C for 5 min. After cooling to room temperature, titanium(IV) butoxide (170 mg) was added to the barium acetate solution, which was then stirred for 1 min. The polymer solution was added dropwise to the barium acetate solution, and then the resulting mixture was spin-coated onto a Si/SiO<sub>x</sub>/Ti/Pt substrate at 3000 rpm for 30 s. After annealing at 120 °C for 5 min, the film was calcined in air at 800 °C for 10 min with a ramp rate of 1 °C·min<sup>-1</sup>. Bulk BT single crystals (Crystal Base, Co., Ltd.) were used as a reference.

First, the synthesized mesoporous BT thin film was characterized by transmission electron microscopy (TEM) and scanning electron microscopy (SEM) using SU-8000 (Hitachi) and H-9000NAR (Hitachi) microscopes, respectively. The surface SEM image confirmed that the synthesized BT thin film contained pores [Fig. 1(a)]. A low-magnification SEM image revealed that neither cracks nor voids were present in the film within an area of several square micrometers. The morphological features of the film in the depth direction were investigated by obtaining cross-sectional TEM images. Large crystallites with lengths of several tens of nanometers were vertically stacked, and the gaps between these crystallites formed pores. The estimated thickness of the BT thin film was around 200 nm [Fig. 1(b)].

To investigate the crystallinity of the BT framework, wide-angle X-ray diffraction (WAXD) measurements were performed on a Rigaku RINT-Ultima III diffractometer using Cu K $\alpha$  radiation. Prominent diffraction peaks of BT were clearly observed, showing that the framework was well crystallized. Unlike in our previous study,<sup>7</sup> diffraction peaks originating from Si-containing by-products were not observed [Fig. 2(a)]. Because a Si/SiO<sub>x</sub>/Ti/Pt electrode was used in this study, the precursor solution was protected from direct contact with Si/SiO<sub>x</sub>. Therefore, no unwanted reaction with Si occurred during the synthesis. The weak peaks at  $2\theta = 22^\circ$ – $32^\circ$  were from BaCO<sub>3</sub> and TiO<sub>2</sub>. BaCO<sub>3</sub> was formed by reaction of BT with atmospheric and/or solvated CO<sub>2</sub>.<sup>8,9</sup> Although BaCO<sub>3</sub> decomposes during thermal treatment in the range of 500–900 °C,<sup>10,11</sup> a small amount of BaCO<sub>3</sub> remained, probably because of the insufficient thermal treatment (800 °C for 10 min). Based on the reactions in an aqueous environment,<sup>9</sup> the proposed formation mechanism of BaCO<sub>3</sub> and TiO<sub>2</sub> is as follows:



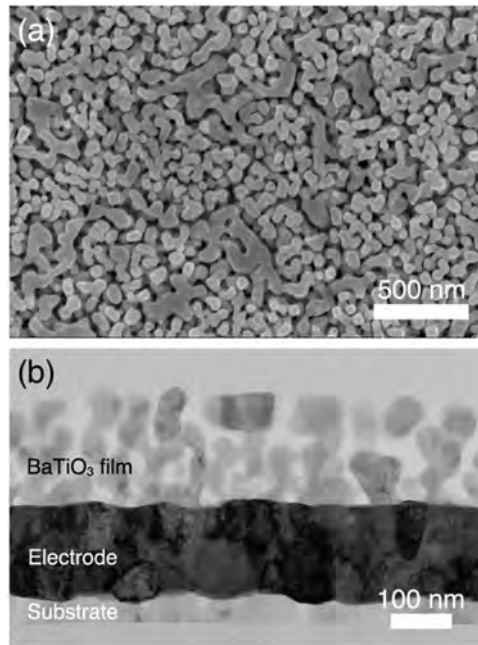


FIG. 1. (a) Top-view SEM and (b) cross-sectional TEM images of the synthesized porous BT thin film.

However, the diffraction peaks of  $\text{BaCO}_3$  and  $\text{TiO}_2$  are much weaker than those of BT. Therefore, the amounts of  $\text{BaCO}_3$  and  $\text{TiO}_2$  are supposed to be much smaller than that of BT.

Although the WAXD pattern confirmed the crystallization of the BT framework, it was still difficult to distinguish between the (ferroelectric) tetragonal and (paraelectric) cubic phases because the WAXD patterns of both phases are similar. The main difference is that the peak at  $2\theta = 45^\circ$  for the cubic phase is split for the tetragonal phase. In this study, detecting such splitting was hard because the peak width was broadened due to the polycrystalline nature of the film.

We employed Raman spectroscopy to investigate the local structural properties in the porous BT thin film [Fig. 2(b)]. Raman spectra of the thin film were collected with an XploRA Plus confocal Raman microscope (Horiba) using an excitation wavelength of 532 nm. In a bulk BT single crystal, characteristic bands at 275, 305, 515, and  $720\text{ cm}^{-1}$  were observed at room temperature, which could

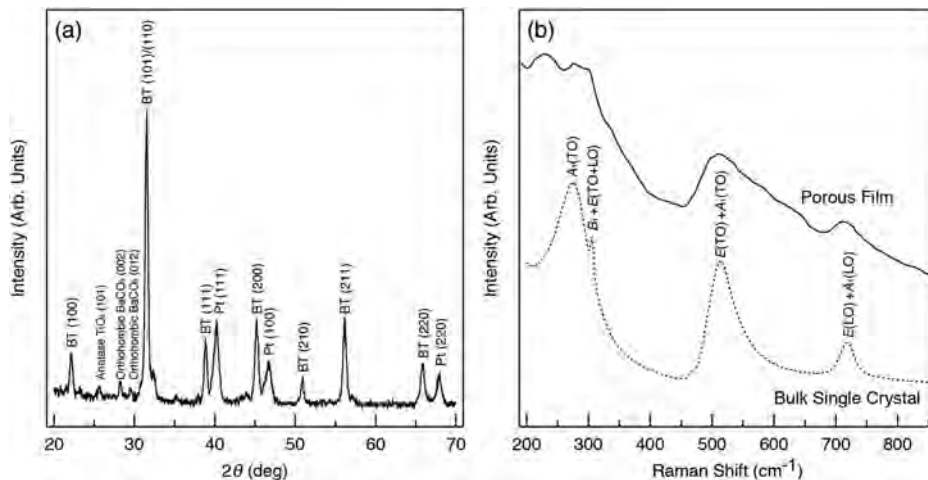


FIG. 2. (a) WAXD pattern and (b) Raman spectrum of the synthesized porous BT thin film measured at room temperature. The prominent peak at  $2\theta = 31.6^\circ$  in the WAXD pattern can be assigned to the (101) or (110) plane of the tetragonal or cubic phase of BT. The Raman spectrum of a bulk BT single crystal is also included as a reference.



be assigned to the  $A_1(\text{TO})$ ,  $B_1 + E(\text{TO} + \text{LO})$ ,  $E(\text{TO}) + A_1(\text{TO})$ , and  $E(\text{LO}) + A_1(\text{LO})$  modes of the tetragonal phase, respectively.<sup>12</sup> In the case of the porous BT thin film, splitting of the  $A_1(\text{TO})$  mode compared with that of the bulk BT single crystal was also confirmed. This change can be attributed to the in-plane compressive stress induced by the interfacial stress. From comparison with high-pressure Raman data, the shift corresponds to an in-plane stress of  $\sim 2$  GPa with respect to that of the bulk BT single crystal. This level of stress is sufficient to achieve stress-induced effects on dielectric/ferroelectric properties.

We also carried out temperature-dependent Raman spectroscopy measurements (Fig. 3). The thin film was heated from room temperature to 525 °C at a ramp rate of 15 °C $\cdot$ min<sup>-1</sup> on a heating stage. The measurements were conducted at three points, and the obtained spectra were averaged. When a bulk single crystal was heated, clear peaks at 305 and 720 cm<sup>-1</sup> disappeared at 140 °C [Figs. 3(a-1) and 3(a-2)]. This is attributed to the phase transition from the (ferroelectric) tetragonal

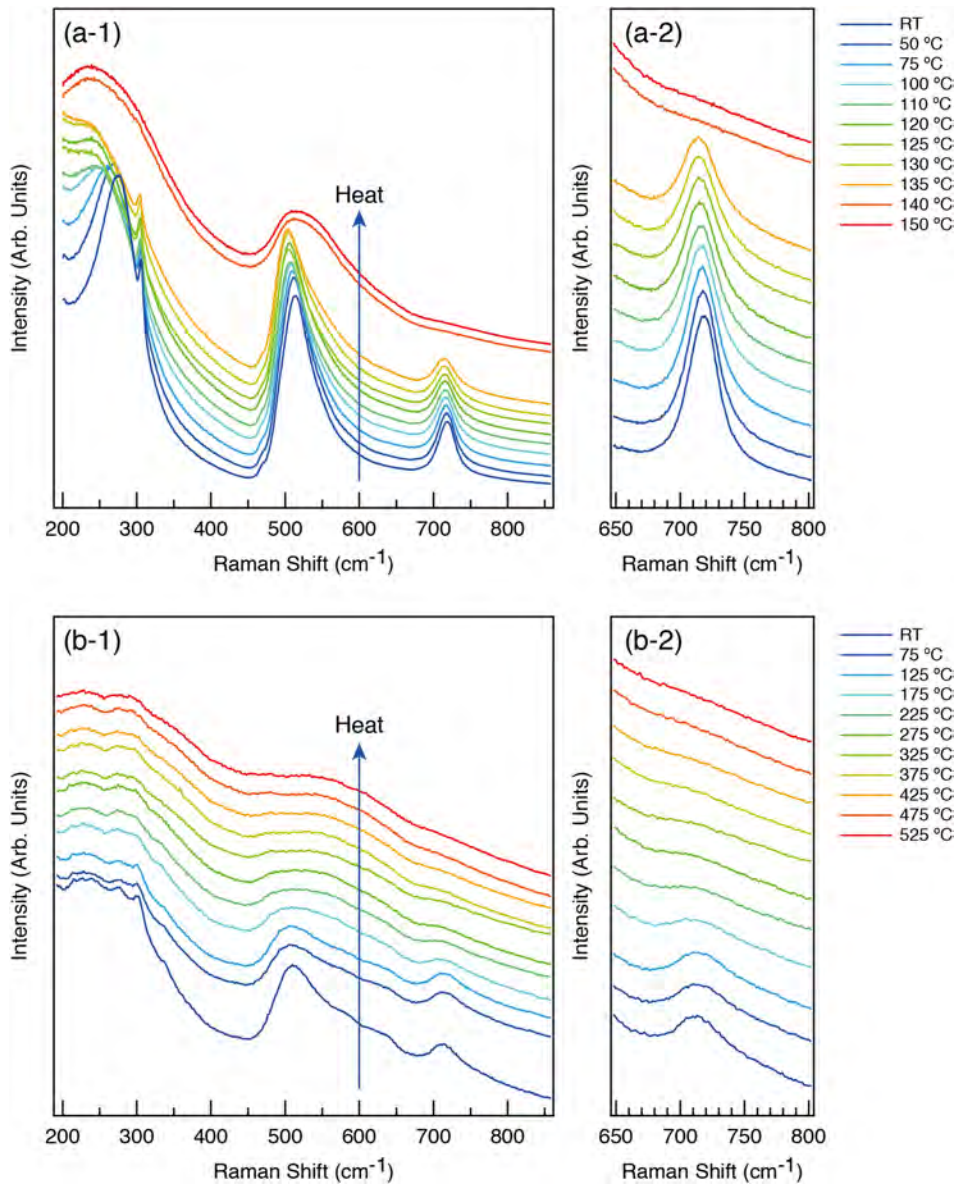


FIG. 3. Temperature dependence of the Raman spectra of [(a-1) and (a-2)] a bulk BT single crystal and [(b-1) and (b-2)] a synthesized porous BT thin film. [(a-2) and (b-2)] is an enlarged image at 650–800 cm<sup>-1</sup>.

to the (paraelectric) cubic phase and is consistent with  $T_C$  of a bulk BT single crystal ( $\sim 130$  °C). In contrast, the peak at  $710\text{ cm}^{-1}$  for the tetragonal phase remained stable to a much higher temperature for the synthesized porous BT thin film. As the temperature rose, this peak gradually became weaker and broader, although it was detectable even at  $375$  °C [Figs. 3(b-1) and 3(b-2)]. This shows that  $T_C$  of the porous BT thin film is much higher than that of the bulk BT single crystal and confirms that the pore-driven stress in the BT thin film is effective at thermally stabilizing the tetragonal phase.

The spatial distribution of stress in the porous BT framework of the thin film was examined by fast Fourier transform mapping (FFTM).<sup>13</sup> Prior to TEM observation, a cross-sectional specimen was prepared by focused ion beam milling. The deformation within the obtained TEM images was visualized by FFTM. FFTM is a method used to analyze and visualize tiny distortions from the FFT patterns of high-resolution TEM images. Figure 4 presents TEM images of areas of the thin film with convex and concave surfaces [Figs. 4(a) and 4(b)] and their corresponding FFTM images [Figs. 4(c)–4(f)]. In FFTM images, we used the “deformation ratio,” which was defined as the ratio of the distances between adjacent atoms deduced by tracking the positions of FFT peaks to the strain-free distance between those atoms. The FFTM image for the  $[1-10]$  direction in a convex area revealed that the outermost convex surface was slightly expanded, which caused lattice relaxation and weakened ferroelectricity. Conversely, the areas below the surface were compressed. Compressed areas clearly

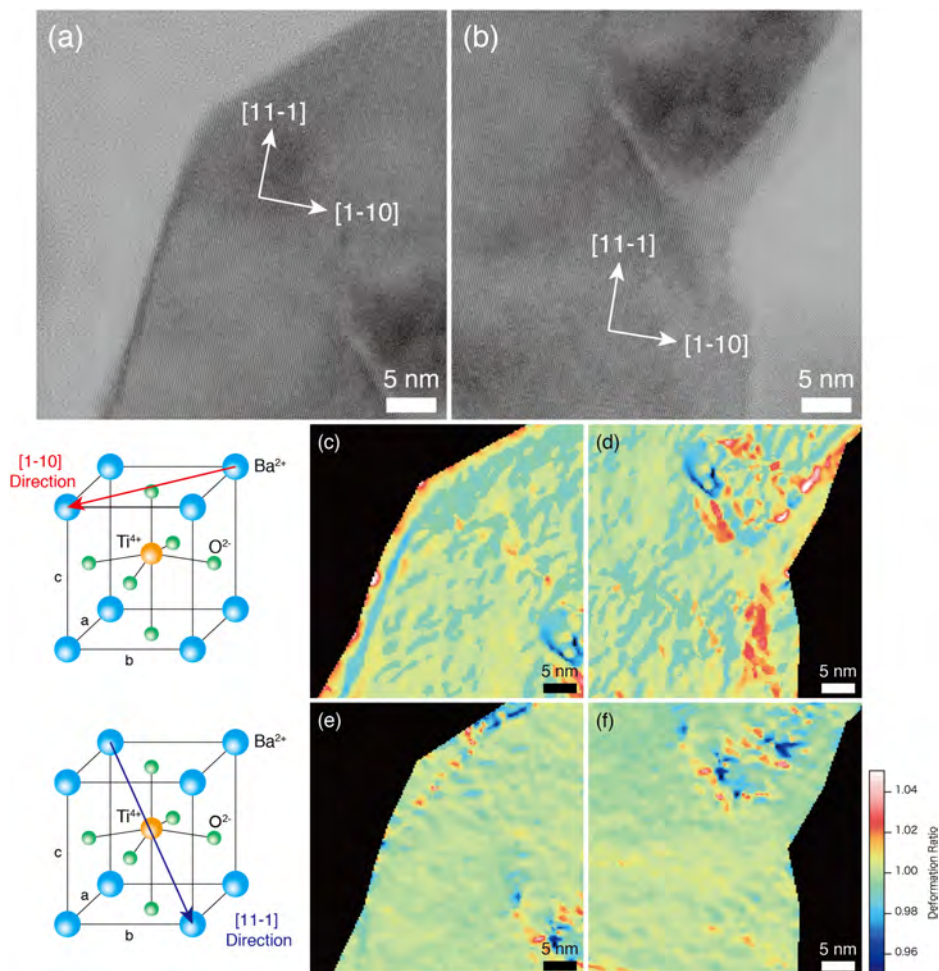


FIG. 4. [(a) and (b)] High-resolution TEM images and [(c)–(f)] FFTM images of [(c) and (e)] convex and [(d) and (f)] concave areas of a porous BT thin film. The orientation of FFTM images is [(c) and (d)]  $[1-10]$  and [(e) and (f)]  $[11-1]$ . In the FFTM images, blue and red parts represent the areas where compressive and tensile stresses are applied, respectively. The orientation used for the analysis is also shown on the left side.



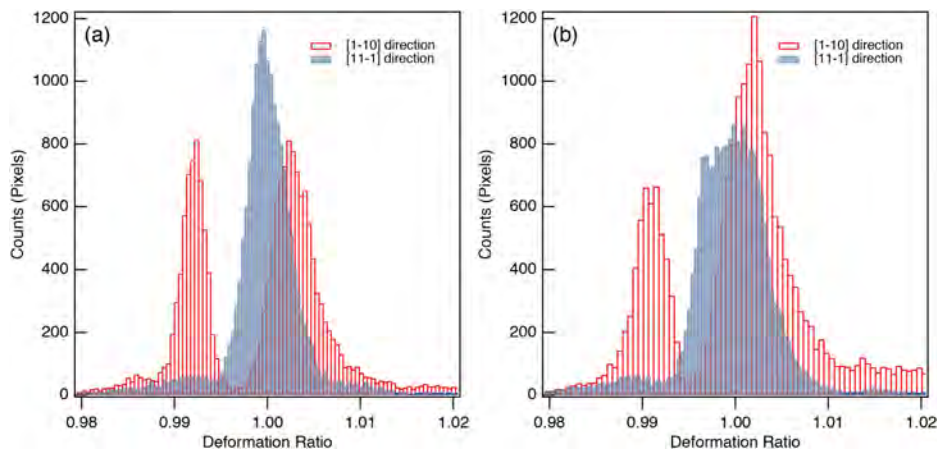


FIG. 5. Histograms of distortion analyzed in (a) convex [shown in Figs. 4(a), 4(c) and 4(e)] and (b) concave [shown in Figs. 4(b), 4(d) and 4(f)] areas of the BT thin film.

appeared inside the framework [Fig. 4(c)]. These findings are consistent with previous work reporting that the surface of a BT nanoparticle was composed of paraelectric cubic phase, while its inner core was the ferroelectric tetragonal phase.<sup>14,15</sup> For concave areas, although deformation of the outermost surface was not clearly observed, probably because the surface was polygonal rather than curved, compression/relaxation was detected in the pore wall [Fig. 4(d)]. In contrast, the FFTM images for the [11-1] direction in both convex and concave areas did not clearly show lattice expansion and contraction [Figs. 4(e) and 4(f)], suggesting that there was little deformation of the BT unit cell in this direction.

To examine the deformation of the BT lattice more quantitatively, the degree of deformation was summarized in the form of histograms (Fig. 5). In the [11-1] direction, the histograms are centered at a deformation ratio of 1 and are nearly symmetrical for both convex and concave areas. This indicates that there was little stress in the [11-1] direction. In contrast, the histograms for the [1-10] direction contained marked peaks at a deformation ratio of around 0.99, indicating areas where compressive stress existed in the BT thin film. These results reveal that anisotropic compressive stress in the [1-10] direction existed in the porous BT thin films. Compressive stress along the [1-10] direction increased the  $c/a$  ratio, causing further displacement of  $\text{Ti}^{4+}$  cations from the center of the lattice. This displacement increased the electric dipole moment of the thin film, which, in turn, enhanced its ferro(piezo)electricity.

In conclusion, we examined the ferroelectricity in a chemically synthesized porous BT thin film. In the Raman spectrum of the thin film, a peak attributed to the (ferroelectric) tetragonal phase at  $\sim 710 \text{ cm}^{-1}$  was observed at room temperature and remained stable until a much higher temperature than  $T_C$  of bulk BT ( $\sim 130 \text{ }^\circ\text{C}$ ). Analyzing high-resolution TEM images of the thin film by the FFTM method revealed compressive stress along the [1-10] direction, which enhanced ferroelectricity because of the increased  $c/a$  ratio (i.e., deformation). These results clarify that the introduction of porosity thermally stabilizes and enhances the ferroelectricity of BT. To fully utilize this effect of porosity, a film should ideally contain densely packed pores. However, during the calcination process to induce crystallization of the BT framework in this study, the porosity decreased because of crystal growth. Therefore, the pore-driven effects on ferroelectricity were limited. To overcome this problem, a novel crystallization process that maintains densely packed pores needs to be developed. Research on this topic is now underway.

This work was financially supported by the Japan Society for the Promotion of Science (JSPS) Grants-in-Aid for Scientific Research (KAKENHI) (Grant No. 26810126). Part of this work (WAXD measurements) was conducted at the Nano-Processing Facility, supported by the Innovation-Boosting Equipment Common (IBEC) Innovation Platform, National Institute of Advanced Industrial Science and Technology (AIST), Japan. Y.Y. and Z.A.A. are grateful to the Deanship of Scientific Research, King Saud University for funding through Vice Deanship of Scientific Research Chairs. This work

was partially supported by the service of The Pore Fabrication Pty Ltd. (Australia) and partial funding from Wollongong City Council (Australia).

- <sup>1</sup> B. Jaffe, W. R. Cook, Jr., and H. Jaffe, *Piezoelectric Ceramics* (Academic Press, London, 1971).
- <sup>2</sup> K. J. Choi, M. Biegalski, Y. L. Li, A. Sharan, J. Schubert, R. Uecker, P. Reiche, Y. B. Chen, X. Q. Pan, V. Gopalan, L.-Q. Chen, D. G. Schlom, and C. B. Eom, *Science* **306**, 1005 (2004).
- <sup>3</sup> V. Nagarajan, C. L. Jia, H. Kohlstedt, R. Waser, I. B. Misirlioglu, S. P. Alpay, and R. Ramesh, *Appl. Phys. Lett.* **86**, 192910 (2005).
- <sup>4</sup> S. C. Wimbush, M. Li, M. E. Vickers, B. Maiorov, D. M. Feldmann, Q. Jia, and J. L. MacManus-Driscoll, *Adv. Funct. Mater.* **19**, 835 (2009).
- <sup>5</sup> S. A. Harrington, J. Zhai, S. Denev, V. Gopalan, H. Wang, Z. Bi, S. A. T. Radfern, S.-H. Baek, C. W. Bark, C.-B. Eom, Q. Jia, M. E. Vickers, and J. L. MacManus-Driscoll, *Nat. Nanotechnol.* **6**, 491 (2011).
- <sup>6</sup> N. Suzuki, M. B. Zakaria, N. L. Torad, K. C.-W. Wu, Y. Nemoto, M. Imura, M. Osada, and Y. Yamauchi, *Chem. - Eur. J.* **19**, 4446 (2013).
- <sup>7</sup> N. Suzuki, X. Jiang, R. R. Salunkhe, M. Osada, and Y. Yamauchi, *Chem. - Eur. J.* **20**, 11283 (2014).
- <sup>8</sup> C. Hérard, A. Faivre, and J. Lemaître, *J. Eur. Ceram. Soc.* **15**, 145 (1995).
- <sup>9</sup> M. C. Blanco López, G. Fournalis, and F. L. Riley, *J. Eur. Ceram. Soc.* **18**, 2183 (1998).
- <sup>10</sup> C. Hérard, A. Faivre, and J. Lemaître, *J. Eur. Ceram. Soc.* **15**, 135 (1995).
- <sup>11</sup> M. A. Delfrate, J. Lemaître, V. Buscaglia, M. Leoni, and P. Nanni, *J. Eur. Ceram. Soc.* **16**, 975 (1996).
- <sup>12</sup> D. A. Tenne and X. Xi, *J. Am. Ceram. Soc.* **91**, 1820 (2008).
- <sup>13</sup> T. Ide, A. Sakai, and K. Shimizu, *Jpn. J. Appl. Phys., Part 2* **37**, L1546 (1998).
- <sup>14</sup> T. Hoshina, S. Wada, Y. Kuroiwa, and T. Tsurumi, *Appl. Phys. Lett.* **93**, 192914 (2008).
- <sup>15</sup> C. Fang, D. X. Zhou, and S. P. Gong, *Phys. B* **406**, 1317 (2011).